

# Fabrication of silica-on-silicon planar lightwave circuits by PECVD and ECR

Libing Zhou (周立兵), Fengguang Luo (罗风光), and Mingcui Cao (曹明翠)

State Key Laboratory of Laser Technology, Huazhong University of Science and Technology, Wuhan 430074

Received November 22, 2004

Plasma enhanced chemical vapor deposition (PECVD) and electron cyclotron resonance (ECR) etching were used in the development of silica layers for planar waveguide applications. The addition of GeH<sub>4</sub> to silica was used to control the refractive index of core layers with core-to-clad index differences in the range of 0.2%—1.3%. Refractive index uniformity variance of  $\pm 0.0003$  was achieved after annealing for 4-inch Si (100) wafers. The core layers with thickness up to 6  $\mu\text{m}$  were etched by ECR with optimized recipe and mask material. Low-loss silica-on-silicon waveguides whose propagation loss is approximately 0.07 dB/cm at 1550 nm are fabricated.

OCIS codes: 130.3130, 230.7380, 160.6030.

Low insertion loss, efficient fiber pigtailed, and high integration density are highly desirable features of devices for optical communication. Materials employed in integrated optics can be classified as either low-contrast type (e.g., doped silica<sup>[1]</sup>, LiNbO<sub>3</sub>) or high-contrast type (e.g., III—V materials). The coupling efficiency of fiber-to-chip is excellent in low-contrast systems<sup>[2]</sup>, but relatively large bend radii are required, leading to a low integration density. High-contrast systems<sup>[3]</sup>, on the other hand, allow very small bending radii and compact devices, but they are difficult to get high-efficiency fiber coupling. Therefore, fabrication of silica waveguide on silicon substrate is especially attractive, and it can take advantage on the well-established semiconductor processing technologies to develop new devices. The silica etching process in planar lightwave circuits (PLCs) is similar to that for semiconductor integrated circuits (ICs), but there is a major difference in the thickness that needs to be etched. The etching depths required for the fabrication of silica waveguide normally exceed 5  $\mu\text{m}$ . The major challenge is to etch patterns on silica layer with clean surface and vertical profile. In the mean time, mask material has to be properly selected to minimize the re-deposition of etching by-products and plasma-induced surface damage.

In this letter, we report the development of low loss plasma enhanced chemical vapor deposition (PECVD) films that demonstrate refractive index control to the uniformity variance of  $\pm 0.0003$ , which is essential in waveguide designs where the calculated tolerances are extremely stringent. The developed 6- $\mu\text{m}$  core layers containing germanium doping exhibit optical losses of approximately 0.07 dB/cm when incorporated into waveguide design. At the same time, in order to increase the etching rate and minimize the surface contamination, high density plasma etching process using electron cyclotron resonance (ECR) with a 13.56-MHz radio frequency (RF) bias and a 2.45-GHz microwave generator has been developed for the PLC fabrication. Commonly, reactive ion etching (RIE) system is used for the waveguide core layer etching, where plasma generated only by a RF discharge has low etching rate, poor etching profile verticality, and rough sidewall in result of low plasma density and severe bombardment with high ion energy.

For an ECR etching system, the plasma was generated mainly by microwave generator, and the ion bias voltage was controlled by the power source. Separating the plasma ion density control (microwave) from the plasma ion energy control (RF bias) results in a highly controllable etching process whereby high plasma density ( $10^{11}$ — $10^{12}$  cm<sup>-3</sup>) and high rate processes at low ion energy (low electron volts) are achieved. An additional benefit of using ECR is its low operating pressure. It results in very high ion mean free paths which ultimately dictate the angle at which an ion impacts the wafer surface, hence further enhancing the anisotropy of the etch and fine sidewall roughness. Operating at such low pressures in a standard RIE chamber would drastically reduce the plasma density and greatly increase the ion energy, totally opposite to the desired effect.

For standard single mode fiber (SMF-28) with 6  $\times$  6 ( $\mu\text{m}$ ) core size, when the refractive index change  $\Delta n = 0.0075$ , the numerical calculation result of high fiber-coupling efficiency of 0.4-dB loss can be reached. The waveguide is fabricated on a standard 4" silicon wafer. The films are deposited by a parallel plate PECVD reactor with a grounded lower electrode and a RF driven upper electrode. The wafer was placed on to the lower electrode, which was heated to 350 °C, giving a substrate temperature of approximately 330 °C. Good grounding contact of the lower electrode is essential for such properties as uniformity and repeatability of refractive index and thickness. A buffer layer of 12- $\mu\text{m}$  thickness ( $n = 1.4508$  at 1546 nm) is deposited using 5%SiH<sub>4</sub>:N<sub>2</sub> and N<sub>2</sub>O as the reactants, followed by the core layer deposition of 6- $\mu\text{m}$ -thick silicon oxide ( $n = 1.4618$  at 1546 nm) using 10%GeH<sub>4</sub>:Ar, 5%SiH<sub>4</sub>:N<sub>2</sub>, and N<sub>2</sub>O. The refractive index contrast between the core and the claddings was adjusted by tuning the 10%GeH<sub>4</sub>:Ar flow rate. After annealing at 1100 °C in oxygen environment for four hours, the Ge-doped oxide core layer is structured in a nickel-masked ECR-process using CHF<sub>3</sub> and O<sub>2</sub> as the etchant. Thereafter, a top cladding layer of the thickness  $\geq 12$   $\mu\text{m}$  is deposited using PECVD under the same conditions as buffer layer deposition.

In PECVD process, RF-induced plasma activation provides thin film decomposition at low operating temperatures because the transfer energy needed for deposition

is obtained from plasma to reactant gases. The discharge ionizes the gases, and creates radicals reacting at wafer surface. The quality of the PECVD deposition of thin films depends strongly on reactor parameters such as RF power, work pressure, temperature, and reactant gas mixture. 5%SiH<sub>4</sub>:N<sub>2</sub> was used as the silicon source for safety and uniformity<sup>[4]</sup>. Pure silane is highly flammable in air which is often undesirable, however silane diluted below its explosion threshold of 4% will not burn in the event of a leak. Nitrous oxide is the preferred oxygen source as silane will not react to it at standard pressures. These ensure the films to have virtually no silica particles/dust.

The waveguide pattern was defined by a nickel layer using standard lithography and wet etching process. In our experiment, an 80-nm nickel masking layer is deposited by sputtering on top of the core layer, and using HF:HNO<sub>3</sub> (1 : 1) mixed wet etchant to define the waveguide pattern on nickel layer after photolithography. Then the waveguide channels are formed by etching in ECR system using CHF<sub>3</sub> and O<sub>2</sub>.

The shape of the waveguide and etched surface morphology can be controlled by changing the etch parameters. The etched profile depends also on the quality of the nickel mask, the reason is that sidewall roughness of the mask layer affects the edge of the waveguide during the ECR etching process. Figure 1 is the scanning electronic microscope (SEM) image of the etched waveguide, and a vertical profile (> 87°) of the edge is shown. A cross section micrograph of the waveguide structures with buffer layer, core layer, and cladding layer is shown in Fig. 2. The film thickness and refractive index were measured using a Metricon Prism Coupler<sup>[5,6]</sup> with a high-resolution stage at 1546 nm, the preferred telecommunication wavelengths. They were based on the 5-point measurement method (C, N, E, S, W, edge exclusion zone 5 mm for 4" wafer). The uniformity variance of film thickness was calculated from (max - min) × 100% / (2 × average)

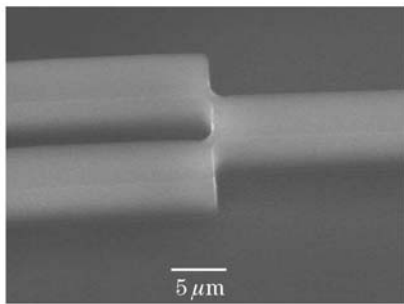


Fig. 1. SEM picture of the core ridge structure of waveguide.

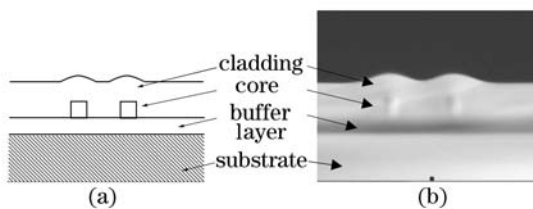


Fig. 2. Scheme (a) and micrograph (b) of a cross section of the waveguide.

and the refractive index from (max - min)/2. Film stress was measured using an FSM128 intelligent film stress measurement system to calculate the difference between pre- and post-process wafer bows.

Figure 3 shows the refractive indices of the buffer layer and cladding layer for various N<sub>2</sub>O:SiH<sub>4</sub> ratios. Results show that the fabricated silicon oxide film can have refractive index ranging from below 1.450 to 1.465.

The conditions of N<sub>2</sub>O:SiH<sub>4</sub> ratio 85 : 1 was chosen for the buffer layer and cladding layer deposition, and based on this we have studied the core layer refractive index varying with the GeH<sub>4</sub> flow rate, as shown in Fig. 4. The graph shows larger refractive index changes after annealing for more highly Ge-doped films. With 40 ml/min of 10%GeH<sub>4</sub>:Ar flow, Δn over the un-doped baseline was 1.5%.

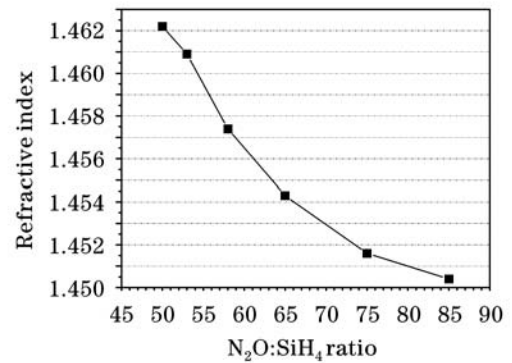


Fig. 3. Refractive index for various N<sub>2</sub>O:SiH<sub>4</sub> ratios.

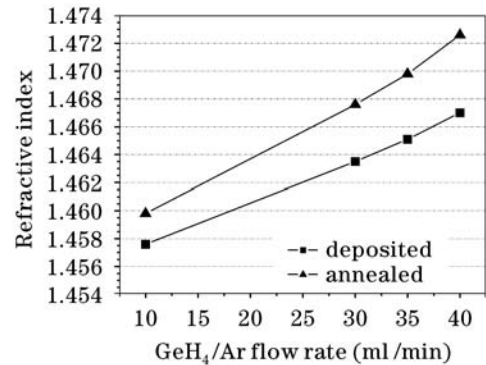


Fig. 4. Refractive index of the film for various GeH<sub>4</sub>:Ar flow rates as deposited and after thermal annealing.

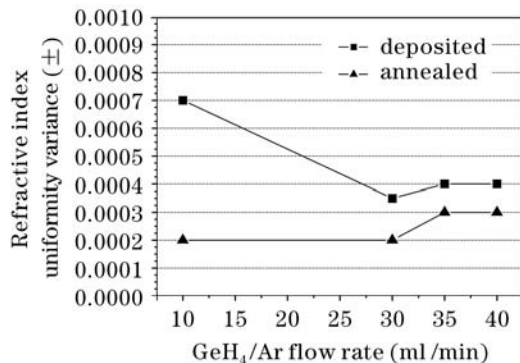


Fig. 5. Refractive index uniformity variance for various GeH<sub>4</sub>:Ar flow rates as deposited and after thermal annealing.

Figure 5 displays the improvements in refractive index uniformity variance that can be achieved after annealing. The uniformity variance for all annealed films is less than  $\pm 0.0003$ , and it is further improved upon annealing. This is unlikely to be due to a reflowing effect as  $\text{SiO}_2$  does not reflow until  $1400^\circ\text{C}$  (or slightly lower with increased Ge content).

The stress of the oxide films is always compressive after annealing. Figure 6 shows how this compressive stress decreases with increasing  $\text{GeH}_4$  flow.

Normally PECVD oxides are in corporate with hydrogen and nitrogen because of the low deposition temperature and the hydrogen-rich precursors silane, nitrogen-rich precursors nitrous oxide<sup>[7]</sup>. An infrared spectrum of the unannealed  $\text{SiO}_2$  waveguide is shown in Fig. 7. The overtones of the O—H and N—H bonds cause the absorption around  $1500\text{ nm}$ .

The removal of O—H and N—H bonds in the annealing process has reduced optical loss. The insertion loss of different length of  $6 \times 6\ (\mu\text{m})$  channel waveguides is measured with the setup consisting of Anritsu MT9810A optical test set and Anritsu ML9001L optical power

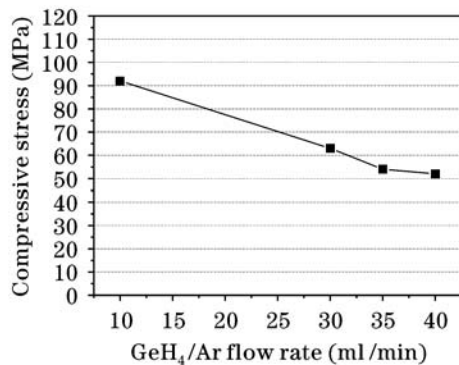


Fig. 6. Stress after annealing of Ge-doped  $\text{SiO}_2$  films.

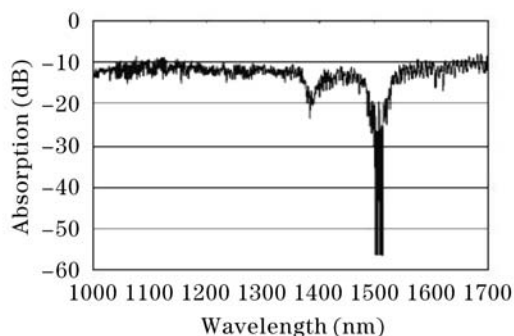


Fig. 7. Absorption spectrum of the unannealed  $\text{SiO}_2$  waveguide.

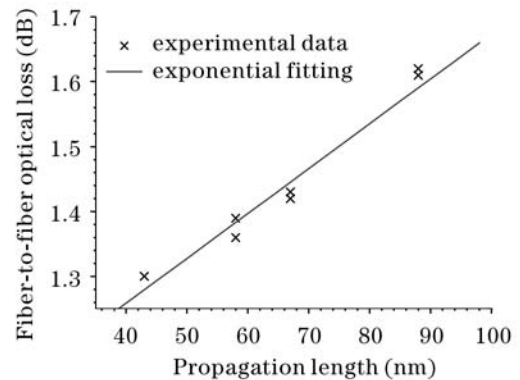


Fig. 8. Fiber-to-fiber optical loss as a function of channel waveguide length.

meter. The relative fiber-to-fiber optical loss as a function of the propagation length in the channel is shown in Fig. 8. From this data, a maximum coupling loss of  $0.5\text{ dB/facet}$  and propagation loss of less than  $0.07\text{ dB/cm}$  are determined.

In conclusion, it has been shown that high quality optical layers that meet the demands of planar waveguides can be produced using PECVD silica doped with germanium. The refractive index uniformity variance of  $\pm 0.0003$  enables the layers to be incorporated into stringent waveguides designs. Annealed films with ECR anisotropic vertically etching can exhibit optical loss of approximately  $0.07\text{ dB/cm}$  measured on fabricated  $\Delta n = 0.75\%$  waveguides.

This work was supported by the National Natural Science Foundation of China under Grant No. 60177023. L. Zhou's e-mail address is libzhou@yahoo.com.

## References

1. M. Kawachi, *Optical and Quantum Electronics* **22**, 391 (1990).
2. S. Suzuki, K. Shuto, H. Takahashi, and Y. Hibino, *Electron. Lett.* **28**, 1863 (1992).
3. K. Kawano, M. Kohtoku, M. Wada, H. Okamoto, Y. Itaya, and M. Naganuma, *IEEE J. Sel. Top. Quantum Electron.* **2**, 348 (1996).
4. S. W. Hsieh, C. Y. Chang, and S. C. Hsu, *J. Appl. Phys.* **74**, 2638 (1993).
5. R. Ulrich and R. Torge, *Appl. Opt.* **12**, 2901 (1973).
6. A. C. Adams, D. P. Schinke, and C. D. Capio, *J. Electrochemical Soc.* **126**, 1539 (1979).
7. L. Martinu and D. Poitras, *J. Vac. Sci. Technol. A* **18**, 2619 (2000).